# 行政院國家科學委員會專題研究計畫成果報告

## 新型非線性光學與寬能帶半導體材料之光電物理性質研究

## Studies on new nonlinear optical materials and wide bandgap semiconductors

計畫編號：NSC 88-2112-M009-035
執行期限：87 年 8 月 1 日至 88 年 7 月 31 日
主持人：謝文峰教授　　國立交通大學光電工程研究所

### 一、中文摘要

本報告研究溶膠凝膠法製備的鈦酸鍶鋇微晶粉末的線性與非線性光學性質。從粉末 X 光繞射、雙折射和二階非線性光學量測的結果顯示，室溫的順電至鐵電相變發生在 $Ba_{0.75}Sr_{0.25}TiO_3$ 的成分。鐵電 BST 的二階非線性光學係數為 7.9 pm/V。折射率為 2.2，雙折率約 0.05，顯示為不錯的非線性光學材料。我們也發現新的排列的秩序相變可能發生於 x 約為 0.4 到 0.5 之間。

關鍵詞：鈦酸鍶鋇、光學材料、溶膠凝膠法、鐵電性、非線性光學性質、相變。

### Abstract

The linear and nonlinear optical properties of sol-gel prepared $Ba_xSr_{1-x}TiO_3$ (BST) crystalline powders were reported. The results from powder x-ray diffraction, birefringence, and second-order optical nonlinearity measurements indicate that the paraelectric-ferroelectric phase transition of $Ba_{0.75}Sr_{0.25}TiO_3$ occurs near room temperature. The second-order optical nonlinearity of the ferroelectric BST is about 7.9 pm/V. The index of refraction, n=2.2, and birefringence, $\Delta n_B$~0.05, are also appropriate for practical nonlinear optical applications. We also found a new order transition may occur at x~0.4-0.5.

Keywords: $Ba_xSr_{1-x}TiO_3$ (BST), optical materials, sol-gel growth, ferroelectricity, nonlinear optical properties, phase transition

### 二、緣由與目的

Ferroelectric materials possess useful properties, which relate to their field-reversible spontaneous polarization below the Curie temperature $T_c$. Two remanant polarizations with opposite polarity are available. The lower frequency transverse optical phonons of some ferroelectrics soften near the ferro-paralectric phase transition [1] and give rise to highly nonlinear dielectric constant. Ferroelectric materials have been widely used in many applications ranging from sensors and actuators [2], new nonvolatile random access memory [3] to various microwave devices such as frequency-agile filters, phase shifters and tunable high Q-resonators [3-5]. An ideal material for these applications must possess high dielectric constant, low dielectric loss, and tunability in material properties.

Ternary and more complex oxides with perovskite structure such as $Ba_xSr_{1-x}TiO_3$ represent an important class of ferroelectric materials, whose electrical properties are tunable with their compositions and structures. Barium titanate ($BaTiO_3$) belongs to the displacement type of ferroelectric material, for which the origin of ferroelectricity derives from the displacement of ions relative to each other with a Curie temperature of 393 $^oK$ [6], while $SrTiO_3$ is paraelectric and never becomes ferroelectric even at $0^oK$. It is known that the dielectric constant of $Ba_xSr_{1-x}TiO_3$ (BST) varies with x=Ba/(Ba+Sr) and becomes anomalously large at the structural phase transition [7]. The mechanism giving rise to the giant dielectric constant has remained unclear. The large dielectric constant of BST thin films can also be tuned with an external electric field, which makes the material attractive for the development of various microwave devices [3].

The electrical properties of BST films had been subjected to detailed investigation, however

little has been done to reveal their optical properties at various compositions [8]. Optical applications with BST are interesting in view that many advanced nonlinear optical devices with BST films can be realized by using periodic poling technique [9,10].

## 三、研究報告應含的內容

*2.1 Preparation of BST powders with a sol-gel method*

Sol-gel technique [11] was employed for preparing $Ba_xSr_{1-x}TiO_3$ crystalline powders in order to yield samples with high composition accuracy. We first boiled acetic acid to 120°C for producing dehydrated solvent. A proper amount of barium acetate and strontium acetate (99% purity from Gransman Inc.) was dissolved in dehydrated acetic acid at 90°C and was sufficiently stirred for 20 min. Titanium isopropoxide and some di-ethanol were then added to the solution and were stirred for another 20 min. We dried and solidified the solution by illuminating with a 400-W infrared lamp for two days. The resulting white solid was heated to 165℃ for an hour and then was ground into powders. We then sintered the powders at 1000 ℃ for 150 min.

The powders were pressed into pellets with a pressure of 10,000 psi and the pellets were sintered again at 1350°C. The surfaces of the resulting pellets were polished for measuring the indices of refraction and powder x-ray diffraction patterns. For powder SHG measurements, the pellets were ground and then sieved to obtain powder samples with particle sizes of 45, 60, 100, 140, 270 and 400 meshes.

*2.2 Linear optical measurement*

To rapidly test and screen a library of new nonlinear optical materials, it is highly desired to develop some simple methods for evaluating the linear and nonlinear optical properties of powder samples.

Stagg and Charampopoulos [12] devised a technique for measuring the index of refraction, $\bar{n} = n - i\kappa$, of a powder sample. They found that the power reflectance from a rough surface at an incident angle, θ, can be described with

$$R(\bar{n}, \theta, \pm/a) = \rho(\theta, \pm/a) R_0(\bar{n}, \theta) \quad . (1)$$

Here $R_0$ represents the reflectance from an ideal smooth surface, and ρ is the scattering factor from surface roughness. Assuming the rough surface can be modeled with a surface profile that follows Gaussian distribution with a root-mean-squared (rms) roughness of σ/λ, the scattering factor can then be derived with Kirchhoff's scalar diffraction theory. For a surface with roughness σ/λ<1 and correlation length $L_c/\lambda<1$, the scattering factor can be simplified to a polarization-independent term [12]

$$\rho(\theta, \pm/a) = \exp[-(4\pi\sigma\cos\theta \pm \frac{\pi}{a})^2]. (2)$$

Therefore, the ratio of two power reflectances with *p*- and *s*-polarized light becomes

$$r = \frac{R_p(\bar{n}, \theta, \pm/a)}{R_s(\bar{n}, \theta, \pm/a)} = \frac{R_{0,p}(\bar{n}, \theta)}{R_{0,s}(\bar{n}, \theta)}. \quad (3)$$

This ratio can be related to the complex index of refraction $\tilde{n} = n - i\kappa$ of material by

$$r = \frac{a^2 + b^2 - 2a\sin\theta\tan\theta + \sin^2\theta\tan^2\theta}{a^2 + b^2 + 2a\sin\theta\tan\theta + \sin^2\theta\tan^2\theta}$$

where

$$2a^2 = \sqrt{(n^2 - \kappa^2 - \sin^2\theta)^2 + 4n^2\kappa^2} + (n^2 - \kappa^2 - \sin^2\theta)$$

and

$$2b^2 = \sqrt{(n^2 - \kappa^2 - \sin^2\theta)^2 + 4n^2\kappa^2} - (n^2 - \kappa^2 - \sin^2\theta) \quad (4)$$

*2.3 Characterization of second-order nonlinear optical properties*

Kurtz and Perry [13] were the first to investigate the second-order NLO responses of crystalline powders. Considering a fundamental beam with wavelength λ normally incidents on a crystal plate with thickness L, the total second-harmonic intensity can be expressed as [14]

$$I_{2\omega} = \frac{128\pi^5 d_{eff}^2 I_\omega^2 L^2}{n_\omega^2 n_{2\omega} \lambda_{2\omega}^2 c} \frac{\sin^2[\Delta kL/2]}{[\Delta kL/2]^2}, \quad (5)$$

where $\Delta k = k(2\omega) - 2k(\omega)$, $I_\omega$ is the intensity of the incident fundamental beam, $n_\omega$, $n_{2\omega}$, and $d_{eff}$ are the indices of refraction and the effective nonlinearity of the crystal plate. When the plate is made with crystalline powders, then the second-harmonic intensity becomes [15]

$$I_{2\omega} = \frac{512\pi^3 I_\omega^2 \bar{l}_c^2}{n_\omega^2 n_{2\omega} \lambda_{2\omega}^2 c} \langle d_{eff}^2 \rangle \frac{L}{\bar{r}} \sin^2[\frac{\pi}{2}(\frac{\bar{r}}{\bar{l}_c})]. \quad (6)$$

Here $\bar{r}$ denotes the averaged particle size, $\bar{l}_c = \langle \lambda_\omega / 4(n_{2\omega} - n_\omega) \rangle$ is the coherent length, and $\langle d_{eff}^2 \rangle$ the square of the effective nonlinearity averaged over the orientation distribution of crystalline powders. When the

second-harmonic generation is not phase matchable, Eq. (6) leads to the following asymptotic forms [15]

$$I_{2\mu} \to \begin{cases} \dfrac{128\pi^5 I_\mu^2}{n_\mu^2 n_{2\mu} \lambda_{2\mu}^2 c}\langle d_{eff}^2\rangle L\cdot \bar{r}, & \bar{r} << \bar{l}_c \\ \dfrac{256\pi^3 I_\mu^2 \bar{l}_c^2}{n_\mu^2 n_{2\mu} \lambda_{2\mu}^2 c}\langle d_{eff}^2\rangle \dfrac{L}{\bar{r}}, & \bar{r} >> \bar{l}_c \cdot \end{cases} \quad (7)$$

If the second-harmonic generation satisfies the type-I phase matching condition, we can rewrite Eq. (5) as [16]

$$I_{2\mu}(\bar{r},\theta) = \frac{128\pi^5\langle d_{eff}^2\rangle I_\mu^2}{n_\mu^2 n_{2\mu} \lambda_{2\mu}^2 c} L\cdot \bar{r} \frac{\sin^2[\frac{\pi}{2}\frac{\bar{r}}{\bar{l}_{pm}}(\theta-\theta_{pm})]}{[\frac{\pi}{2}\frac{\bar{r}}{\bar{l}_{pm}}(\theta-\theta_{pm})]^2}, \quad (8)$$

where $\bar{l}_{pm} = \lambda_\mu / [4|\Delta n_{B,2\mu}|\sin 2\theta_{pm}]$, and $\theta_{pm}$ is the phase matching angle. Here $\Delta n_{B,2\mu} = n_{E,2\mu} - n_{O,2\mu}$ denotes the birefringence of material at the second-harmonic wavelength. In the event that $\bar{r} \ll \bar{l}_{pm}$ or $\bar{r} \gg \bar{l}_{pm}$, Eq. (8) can be simplified to

$$I_{2\mu} \to \begin{cases} \dfrac{256\pi^4 I_\mu^2}{n_\mu^2 n_{2\mu} \lambda_{2\mu}^2}\langle d_{eff}^2\rangle L\cdot \bar{l}_{pm}, & \bar{r} >> \bar{l}_{pm} \\ \dfrac{128\pi^5 I_\mu^2}{n_\mu^2 n_{2\mu} \lambda_{2\mu}^2}\langle d_{eff}^2\rangle L\cdot \bar{r}, & \bar{r} << \bar{l}_{pm} \cdot \end{cases} \quad (9)$$

We derived a useful empirical formula, which possesses the correct asymptotic forms in Eq. (9), to depict the overall variation in second harmonic intensity with particle size $\bar{r}$

$$I_{2\mu} = I_0\sqrt{1-\exp[-(\bar{r}/A)^2]}$$

$$with\ I_0 = \frac{256\pi^4 I_\mu^2}{n_\mu^2 n_{2\mu} \lambda_{2\mu}^2 c} L\bar{l}_{pm} < d_{eff}^2 > \cdot \quad (10)$$

$$and\ A \approx 9\,\bar{l}_{pm}$$

An experimental arrangement for measuring the second-harmonic scattering pattern from crystalline powders is described in Fig. 1. In this setup, the fundamental beam normally incidents on the sample cell. A liquid light guide with its input end attached on a rotation stage is employed to collect the second harmonic intensity at various scattering angles. We can integrate the second harmonic pattern over scattering angle to yield the total second harmonic intensity, $I_{2\omega}$.

## 四、結果與討論

### *3.1 Structural determination of $Ba_xSr_{1-x}TiO_3$ with powder X-ray diffraction*

We first employ x-ray diffraction (XRD) for probing the unit cell dimensions of $Ba_xSr_{1-x}TiO_3$ with various x-values. The resulting XRD patterns were then analyzed with Rietvelt refinement procedure [17]. In Fig. 2, the XRD patterns from four powder samples (x = 1, 0.8, 0.5, and 0, from top to bottom) are presented. The averaged cell dimension as a function of x is summarized in Fig. 3.

The unit cell of our synthesized $BaTiO_3$ crystalline powder has an averaged dimension of $(a+c)/2 = (3.986+4.020)/2 = 4.003$ Å. The data agrees well with the published results, where $a$ is found to range from 3.9915 to 3.9998 Å and $c$ from 4.018 to 4.025 Å) [18]. For $SrTiO_3$, our measured result ($a=b=c=3.897$ Å) is slightly smaller than the published data ($a$ varies from 3.900 to 3.905 Å) [18], but the difference is within our experimental error. It can also be seen that Vegard's linear scaling law [8] is not satisfied but a square law with a jump around x~0.4-0.5. This jump may be attribute to ordering phase transition.

### *3.2 Linear optical properties of $Ba_xSr_{1-x}TiO_3$*

To estimate the measuring accuracy of index of refraction from Eq. (4), we first apply this linear optical technique on some well-known NLO materials. The results of $KH_2PO_4$ (KDP) crystalline powder at $\lambda$=0.633 μm are presented in Fig. 4. By using Eq. (4), the index of refraction of KDP was determined to be 1.49, which is fairly close to the averaged value of $n_E$ and $n_O$ of KDP single crystal (see Table I) [19].

We then apply this method to probe linear optical properties of BST powders with various Ba/(Ba+Sr) ratios. The results show the index of refraction of BST is fairly constant (~2.20). The value is about 8% lower than that taken from single crystal $BaTiO_3$ ($n_{av}$=2.39) and $SrTiO_3$ (n=2.39) [20]. The deviation is most likely originated from larger light scattering loss from our powder samples.

### *3.3 Nonlinear optical properties of $Ba_xSr_{1-x}TiO_3$*

For calibration, the nonlinear optical (NLO) characterization apparatus described in

Fig. 1 was first applied to investigate NLO responses of KDP and β-$BaB_2O_4$ (BBO) powders. The results show that second harmonic generation from these two standard materials is phase matchable at 1.06 μm. The NLO response from BBO is about four times of KDP, which agrees very well with the published values [19].

We then apply this experimental setup to measure NLO properties of BST powders. The results are shown in Fig. 5. The second harmonic generation from BST is also phase-matchable at 1.06 μm. The effective second-order nonlinearities of $Ba_xSr_{1-x}TiO_3$ with x=0.8 and 0.7 were found to be about 7.2 pm/V and 3.5 pm/V, respectively. The effective nonlinearities, $\sqrt{\langle d_{eff}^2 \rangle}$, and birefringence, $\Delta n_B = n_{E,2\omega} - n_{O,2\omega}$, of BST with various x are summarized in Fig. 6. It is interesting to note that the $\sqrt{\langle d_{eff}^2 \rangle}$ and $\Delta n_B$ exhibit a discontinuous change with x=0.75 and x~0.45. This supports that BST with Ba/(Ba+Sr)~0.75 undergoes a structural phase transition near room temperature and ordering transition at x~0.45.

## 五、結論

As pointed out previously that barium titanate ($BaTiO_3$) belongs to the displacement type of ferroelectric material for which the origin of ferroelectricity derives from the displacement of ions relative to each other. It is believed that BST undergoes the same sequence of structural phase transitions as that pure $BaTiO_3$ does, but at progressively lower phase transition temperatures as the concentration of Ba is reduced. The Ti-$O_6$ octahedron in the ferroelectric $BaTiO_3$ is distorted with $C_{4v}$-symmetry. The resulting spontaneous polarization, $P_s$, can be expressed as [21]

$$P_s = P_0' \cdot \Delta z, \qquad (11)$$

where Δz denotes the displacement of ions from the symmetric positions which are occupied in the paraelectric phase. $P_s$ serves as an order parameter of the phase transition and therefore above the transition the parameter varies with temperature by [22]

$$P_s = a\sqrt{T_c - T}. \qquad (12)$$

Recently, Wang [23] had proposed a simple two-band model suited for describing polarization in a ferroelectric crystal. With the model, the second-order NLO coefficient of a ferroelectric crystal had been derived to be

$$d_{eff} = \frac{®C(n_\mu^2 + 2)^2 E_0^6}{18(E_0^2 - \eta^2\mu^2)^2(E_0^2 - 4\eta^2\mu^2)} P_s. \qquad (13)$$

Here $E_0$ is the energy gap of the ferroelectric material and $C$ denotes a simple constant. By combining Eqs. (11) and (13), we then have

$$d_{eff} = d' \cdot \Delta z. \qquad (14)$$

Note that the displacement of ions may lead to a change in unit cell dimension. Based on the model, birefringence can also be related to spontaneous polarization by $\Delta n_B = B \cdot P_s^2$ [23]. Therefore, we are expecting to observe that both the second-order optical nonlinearity and birefringence vary with the mole fraction of Ba. Indeed, this is what we have observed shown in Fig. 6.

We should point out that the linear optical dispersion from 1.064 μm to 0.532 μm in a single crystal $BaTiO_3$ is about 0.13 [20], which is larger than the birefringence ($\Delta n_B$=-0.06). Therefore the type-I phase matching condition should not be satisfied in $BaTiO_3$ at 1.064 μm. However, note that single crystal $BaTiO_3$ usually contains various transition metal impurities, which often results in red shift of the absorption edge. Our BST crystalline powders prepared with sol-gel method do not contain such unintended dopants. Therefore our samples more accurately reflect the intrinsic properties of the materials and possess smaller dispersion in the visible light spectrum region. This can lead to the observed type-I phase matched second-harmonic generation in BST shown in Fig. 5.

Note that the index of refraction at the zero frequency limit ($\eta\mu << E_0$) can be expressed as [24]

$$n^2 = 1 + \frac{8®e^2\eta^2}{m^2 V} \sum_k \sum_{vc} \frac{p_{vc}(k) p_{cv}(k)}{E_{cv}^3(k)}. \qquad (15)$$

It is dominated by those interband transitions which lie near band gap (smaller $E_{cv}$) and possess large momentum matrix elements, $p_{cv}$. In BST, oxygen's $2p$ and titanium's $3d$ orbitals dominate these transitions, where Ba and Sr do not play an important role. This lead to that the index of refraction of BST should be irrelevant to the concentration of Ba. Indeed this exactly agrees with our observation. It should be pointed out that Ba/Sr play the major role in causing unit cell distortion, which more sensitively reflects in

second-order optical nonlinearity and birefringence.

The birefringence of BST shown in Fig. 7 varies from 0.03 to 0.06 as the mole fraction of Ba is increased from 0 to 1. Note that to achieve high conversion efficiency both of the phase matching condition ($\Delta k = 0$) and large angular acceptance ($\phi \approx 0.443 \lambda / (L \cdot |\Delta n_B|)$) have to be achieved. The measured linear and nonlinear optical properties of BST warrant a high efficacy in second-order nonlinear optical applications.

In summary, we investigate linear and nonlinear optical properties of $Ba_xSr_{1-x}TiO_3$ with various mole fractions of Ba. Our results indicate ferroelectric BST possess an effective second-order nonlinearity of about 7.9 pm/V, which is comparable to $LiNbO_3$. In addition, the index of refraction, n=2.2, and birefringence, $\Delta n_B$~0.05, are also appropriate for practical NLO applications. By combining with their excellent electrical and mechanical characteristics, BST could serve as an ideal multifunctional, smart material in micro optical electro-mechanical systems (MOEMS) [25.26]

## 六、自我評估

**本年度中我們以溶膠凝膠法製備一系列鈦酸鍶鋇的微晶粉末，並以 X 光繞射、折射率和粉末二倍頻量測，發現除了結構相變發生在 x=0.75 與文獻相符外，在 x~0.45 時新發現排列秩序相變。進行中的拉曼與紅外光譜研究生子再相變時軟化希望進一步確定這個相變與結構相變對光學與非線性光學性質之影響。**

## 七、參考文獻


[1] E. C. S. Tavares, P. S. Pizani, and J. A. Eiras, Appl. Phys. Lett. 72, (1998) 897.

[2] J. M. Herbert, *Ferroelectric Transducers and Sensors* (Gordon and Breach, London, 1982).

[3] J. F. Scott, Ferroelectrics Rev. 1, (1998) 1.

[4] L. A. Knauss, J. M. Pond, J. S. Horwitz, and D. B. Chrisey, Appl. Phys. Lett. 69, (1996) 25.

[5] P. Bhattacharya, T. Komeda, K. Park, and Y. Nishioka, Jpn. J. Appl. Phys., Part 1 32, (1993) 4102.

[6] H. P. Roaksby and H. D. Megaw, Nature 155, (1945) 484.

[7] F. N. Bunting, G. R. Shelton, and A. S. Creamer, J. Am. Ceram. Soc. 30, (1947) 114.

[8] P. Pasierb, S. Komornicki, and M. Radecka, Thin Solid Film 324, (1998) 134.

[9] L. E. Myers, G. D. Miller, R. C. Eckardt, M. M. Fejer, R. L. Byer and W. R. Bosenberg, Opt. Lett. 20, (1995) 52.

[10] H. Karisson, F. Laurell, L. K. Cheng, Appl. Phys. Lett. 74, (1999) 1519.

[11] L. L. Hench and J. K. West, Chem. Rev. 90, (1990) 33072.

[12] B. J. Stagg and T. T. Charalampopoulos, Appl. Opt. 30, (1991) 4113.

[13] S. K. Kurtz and T. T. Perry, J. Appl. Phys. 39, (1968) 3798.

[14] R. W. Boyd, *Nonlinear Optics* (Academic Press, Boston, 1992).

[15] A. Graja, Acta Physica Polonica A37, (1970) 539.

[16] P. N. Prasad and D. J. Williams, *Introduction to Nonlinear Optical Effects in Molecules and Polymers* (John Wiley and Sons, Inc., N.Y., 1991), Chap. 6.

[17] A computer program for Rietveld analysis of x-ray and neutron powder diffraction patterns, by C.J. Howard and B.A. Hunter, February 1997, Australian Nuclear Science and Technology Organization, Lucas Heights Research Laboratories, Private Mailbag 1, Menai 2234, N.S.W., Austalia.

[18] For $BaTiO_3$ (P4MM) see, for example, R. Waesche, W. Denner, H. Schulz, Mater. Res. Bull. 16, (1981) 497; and R. H. Buttner, E. N. Maslen, Acta Crystallographica B 48, (1992) 764. For $SrTiO_3$ (PM-3M): Yu A. Abramov, V. G. Tsirelson, V. E. Zavodnik, S. A. Ivanov, and I. D. Brown, Acta Crystallographica B 51, (1995) 942; and S. A. Howard, J. K. Yau, H. U. Anderson, J. Appl. Phys. 65, (1989) 1492; for BST ceramics see M. McQuarrrie, J. Am. Ceram. Soc. 38 (1955) 444.

[19] V. G. Dmitriev, G. G. Gurzadyan, and D. N. Nikogosyan, *Handbook of Nonlinear Optical Crystals*, Springer Series in Optical Sciences Vol. 64 (Springer-Verlag, Berlin, 1991).

[20] E. D. Palik, *Handbooks of Optical Constants of Solids II*, (Academic Press, Inc., San Diego, CA, 1991), pp. 789-804 and pp. 1035-1048

[21] W. Zhong, R. D. King-Smith, and D. Vanderbilt, Phys. Rev. Lett. 72, (1994) 3618.

[22] G. A. Smolensky, J. Phys. Soc. Japan, Suppl. 28, (1970) 26.

[23] F. Wang, Phys. Rev. B59, (1999) 9733.

[24] B. Adolph, V. I. Gavrilenko, K. Tenelsen, F. Bechstedt, and R. Del Sole, Phys. Rev. B53,

(1996) 9797.
[25] A. W. Sleight, J. L. Gillson, P. E. Bierstedt, Solid State Commun. 17, (1975) 27.
[26] P. F. Baude, C. Ye, and D. L. Polla, Appl. Phys. Lett. 64, (1994) 2670.

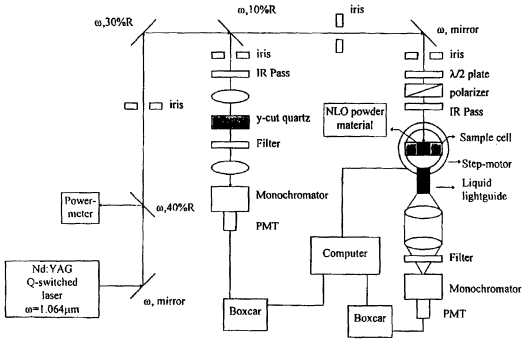


**Fig. 1** Experimental set-up used for measuring second harmonic scattering pattern from a crystalline powder sample.

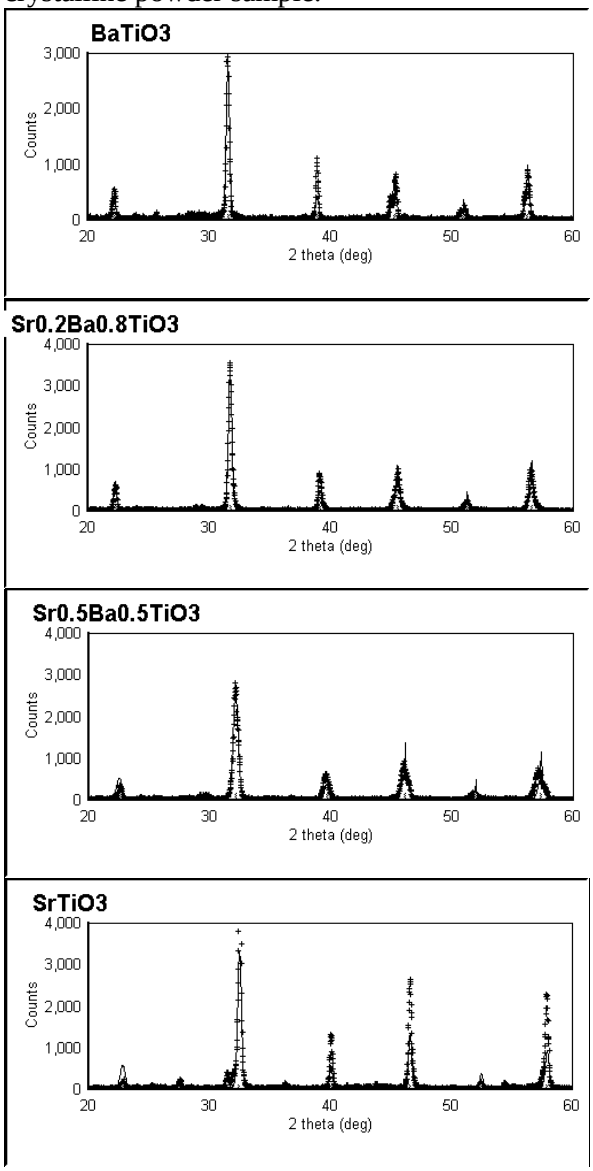


**Fig. 2** Powder x-ray diffraction patterns (symbols) of $Ba_xSr_{1-x}TiO_3$ with x=1, 0.8, 0.5, and 0 (from top to bottom). The solid curves are resulted from the Rietvelt refinement procedure.

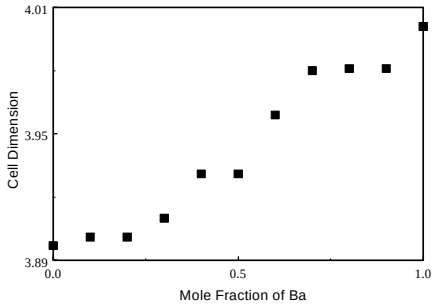


**Fig. 3** Averaged unit cell dimension, $(a+c)/2$, deduced from the Rietvelt refinement procedure is plotted as a function of x. The point group symmetry of the unit cell is taken to be $C_{4v}$ for $x \geq 0.75$ and $O_h$ for $x < 0.75$.

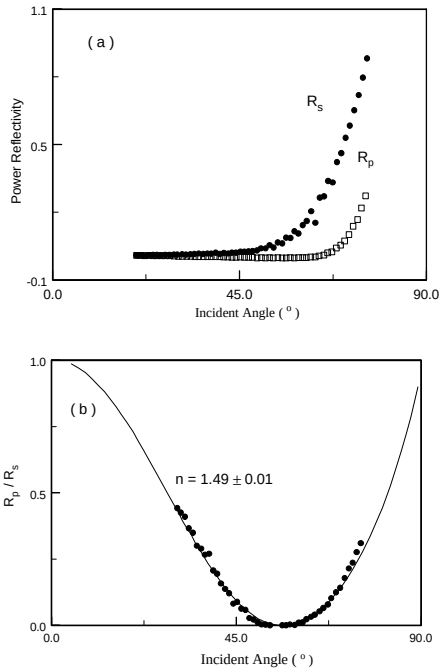


**Fig. 4** (a) Power reflectances with *s*- (filled symbols) and *p*-polarized (open squares) beams as a function of incident angle from a KDP powder pellet; (b) The ratio of the power reflectances with the *p*-polarized to *s*-polarized incident beams is presented (symbols). The solid curve is the theoretical fit to Eq. (4) with n=1.49 and $\mathcal{C} = 0$.

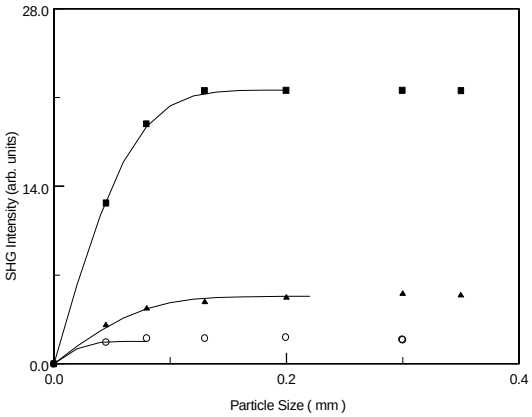


Fig. 5 **Effective second-order optical nonlinearities of BBO (open circles), $Ba_xSr_{1-x}TiO_3$ (x=0.7, filled triangles) and $Ba_xSr_{1-x}TiO_3$ (x=0.8, filled squares) are plotted as a function of particle size. The solid curves are the theoretical fit to Eq. (10).**

**Fig. 6** The measured $\sqrt{\langle d_{eff}^2 \rangle}$ and $\Delta n_B$ of $Ba_xSr_{1-x}TiO_3$ are plotted as a function of x.